arXiv:1402.2906v1 [cs.AR] 12 Feb 2014

TRIAD: A Triple Patterning Lithography Aware Detailed Router

Yen-Hung Lin[1],Bei Yu[2], David Z. Pan[2], and Yih-Lang Li[1]
[1] Department of Computer Science, National Chiao Tung University, Hsinchu, Taiwan
[2] Department of ECE, University of Texas at Austin, Austin, TX, USA
homeryenhung@gmail.com, bei@cerc.utexas.edu, dpan@ece.utexas.edu, ylli@cs.nctu.edu.tw

***Abstract*—TPL-friendly detailed routers require a systematic approach to detect TPL conflicts. However, the complexity of conflict graph (CG) impedes directly detecting TPL conflicts in CG. This work proposes a token graph-embedded conflict graph (TECG) to facilitate the TPL conflict detection while maintaining high coloring-flexibility. We then develop a TPL aware detailed router (TRIAD) by applying TECG to a gridless router with the TPL stitch generation. Compared to a greedy coloring approach, experimental results indicate that TRIAD generates no conflicts and few stitches with shorter wirelength at the cost of 2.41× of runtime.**

I. Introduction

As manufacturing process node enters the nano-meter era, the gap between the illumination wavelength of 193*nm* and the target process node becomes increasingly larger. The semiconductor industry encounters the limitation of manufacturing sub-22*nm* due to the delay of the next generation lithograph (NGL) such as extreme ultraviolet (EUV) and E-beam direct write [1]. To bridge the gap, double patterning lithography (DPL) is adopted, which decomposes a single layer into two masks (colors) to increase the pitch and enhance the resolution [2].

Deploying DPL involves two challenges. *Layout decomposition* requires assigning two features to opposite colors (masks) if their spacing is less than a specific spacing, denoted as sp_{dp}. One *coloring conflict* occurs when two features whose spacing is less than sp_{dp} cannot be assigned to different masks. *Stitch generation*, as the second challenge, is used to solve the coloring conflicts at the cost of yield loss due to the high sensitivity of stitches due to the overlay error. However, some coloring conflicts cannot be solved even after the stitch generation, e.g., native conflicts. Figure 1 shows that one un-decomposable layout (Fig. 1(a)) becomes decomposable after generating one stitch (Fig. 1(b)). Figure 1(c) depicts one layout containing native conflicts in which the spacing between arbitrary two features is less then sp_{dp}.

To further shrink the process nodes below 22*nm*, the paradigm of DPL can be extended to the triple patterning lithography (TPL) to compensate the delay of NGL. If single exposure half-pitch is about 40*nm*, the 193*nm* lithography could be used to manufacture the 11*nm* process node [3]. Compared to DPL, TPL contains one additional mask and can easily solve the native conflicts of DPL. In the example of Fig. 1(c), TPL assigns the three features to three masks, respectively.

Successfully carrying out the layout decomposition requires layouts containing no native conflicts. Considering DPL in the layout synthesis, especially in the detailed routing stage, facilitates generating layouts without native conflicts. Cho *et al.* [4] developed the first DPL-friendly detailed routing approach which greedily determined the masks of routed wire segments to avoid generating layouts with native conflicts. Gao and Macchiarulo [5] proposed lazy color decision and last conflict segment recording to enhance the DPL-aware detailed routing based on [4]. Lin and Li [6] developed a deferred coloring assignment-based gridless detailed routing flow to escape from the suboptimum that may be reached by adopting the greedy coloring strategy. Yuan and Pan [7] spread wires to simultaneously minimize the number of conflicts and stitches, while introducing as less the layout perturbation as possible. On TPL, previous researches only focus on the layout decomposition. Cork *et al.* [8] applied a SAT solver to decompose layouts into three colors. Bei *et al.* [9] proposed a novel vector programming formulation for TPL decomposition and applied a semidifinite programming (SDP) to solve the problem effectively. Chen *et al.* [10] and Mebarki *et al.* [11] proposed a self-aligned triple patterning (SATP) process to extend the 193*nm* immersion lithography to half-pitch 15*nm* patterning.

Similar to DPL, generating TPL-friendly layouts, especially in the detailed routing stage, becomes urgent as TPL is being considered and adopted in the industry [12]. Generating TPL-friendly layouts is more difficult than the TPL layout decomposition while the TPL decomposition has been shown as a NP-complete problem [9]. The DPL coloring conflicts can be easily detected by finding an odd-length cycle in a conflict graph (CG) [13] [6] [5], which cannot be applied to detect TPL coloring conflicts. The greedily coloring approach such as [4] can be directly applied to generate TPL-friendly layouts. However, greedily determining the colors of routed wire segments significantly sacrifices the flexibility of coloring assignment, which may result in generating native conflicts and introducing unnecessary stitches. Moreover, the complexity of CG impedes directly detecting TPL coloring conflicts with high flexibility of coloring assignment in one CG. Figure 2(a) depicts one layout with eight features. One greedy coloring approach sequentially colors features (A, B, C, D,

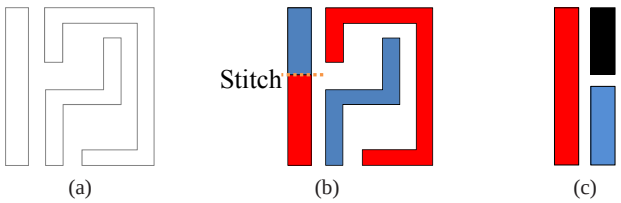

Figure 1. Challenges of DPL: (a) layout cannot be directly decomposed into two masks; (b) layout becomes decomposable after splitting one feature by generating one stitch; (c) layout contains native conflict.

This paper is supported in part by NSF under projects 0644316 and 1218906, NSC of Taiwan 101–2220–E–009–043, NSF of China 61128010, IBM, Intel, Oracle, and Synopsys.
Permission to make digital or hard copies of all or part of this work for personal or classroom use is granted without fee provided that copies are not made or distributed for profit or commercial advantage and that copies bear this notice and the full citation on the first page. To copy otherwise, to republish, to post on servers or to redistribute to lists, requires prior specific permission and/or a fee.
IEEE/ACM International Conference on Computer-Aided Design (ICCAD) 2012, November 5–8, 2012, San Jose, California, USA
Copyright©2012 ACM 978-1-4503-1573-9/12/11 ...$15.00.

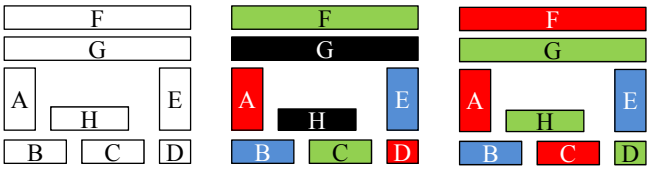

Figure 2. Effects of coloring ordering to TPL coloring result: (a) layout contains eight features; (b) sequentially coloring (A, B, C, D, E, F, G, H) with colors (c_1, c_2, c_3, c_1, c_2, c_3, c_1, c_2) causes G and H un-colorable; (c) coloring result without conflicts exists.

E, F, G, H) in Fig. 2(a) with colors (c_1, c_2, c_3, c_1, c_2, c_3, c_1, c_2). Figure 2(b) displays the coloring result, in which G and H become un-colorable. Nevertheless, the layout can be colored without any un-colorable feature as shown in Fig. 2(c). Therefore, a TPL conflict detection with *high coloring-flexibility* and *low detection-complexity* is desired in a correct-by-construction approach.

In this work, a *token graph-embedded conflict graph* (TECG), comprising a token graph (TG) and a conflict graph (CG), is proposed to enable detailed routers to generate TPL-friendly layouts by a correct-by-construction approach. One TG is used to maintain the coloring relation among different vertex sets in one CG. In one TG, one *strictly colored component* (SCC) is constructed to fix the coloring relation among certain vertex sets in one CG. We apply the proposed TECG to a detailed routing model [14] [15] to implement a *triple patterning lithography aware detailed router* (TRIAD). During the path searching, TRIAD adopts the TECG to detect if any TPL conflict occurs by the current routing wire segment. After detecting solvable TPL conflicts, TRIAD utilizes the TECG to generate stitches in wire segments. With the assistance of TECG, TRIAD can generate stitches which cannot be generated by adopting the conventional DPL stitch generation scheme. Notably, the TPL stitch generation scheme can split one wire segment into several segments even when the wire is entirely intersected by the TPL effect regions of other wire segments.

The main contribution of this paper is to realize a TPL aware detailed router TRIAD with the following two novel techniques:

- A TECG is proposed to assist detailed routers in detecting the TPL conflicts in a correct-by-construction approach while keeping high coloring-flexibility.
- A TPL stitch generation scheme is proposed to generate stitches which may not be generated by adopting the conventional DPL stitch generation scheme.

The remainder of the paper is organized as follows: Section II presents the basic concepts and the problem formulation. Sections III and IV introduce the proposed TECG and TRIAD, respectively. Next, Section V summarizes the experimental results. Brief conclusions are drawn in Section VI.

II. Preliminaries and Problem Formulation

A. Conflict Graph

Kahng *et al.* [13] first adopted a conflict graph (CG) to maintain the relationship among wire segments for the DPL layout decomposition. A vertex in one CG represents one wire segment in a layout. An edge between two vertices, v_i and v_j, in one CG is generated when the minimum spacing between the wire segments represented by v_i and v_j is smaller than minimum coloring spacing, denoted as sp_{dp}. One DPL coloring conflict occurs when there is an odd number of connected vertices in a cycle in one CG.

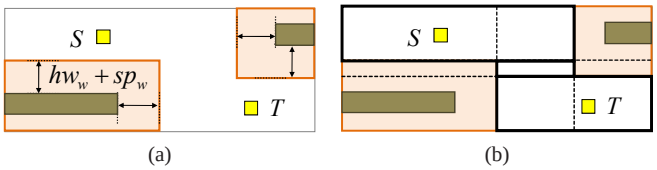

Figure 3. Routing graph construction of NEMO [14] [15]: (a) contour generation for each routed wire; (b) routing graph construction and PMT extraction.

B. Routing Model

The detailed routing can be classified into grid-based one and gridless one based on the utilized routing models. While utilizing the routing resources in a dense layout better than the conventional grid-based routers do, the gridless routers construct more complex data structures than grid-based routers owing to the ability to accommodate the routing rules in the routing graph. Besides, to fit the demand of regular layout designs, gridless routers can also generate on-grid routing wires with an on-grid feature. Two conventionally adopted gridless routers are tile-based one and implicit connection graph-based one, which possess the advantages of low path propagation complexity and fast routing graph construction, respectively [16] [17].

NEMO [14] [15] is an implicit connection graph-based router with both the benefits of tile-based and implicit connection graph-based routers. Before each routing, NEMO expands each obstacle and routed net by half of a wire width hw_w and one wire spacing sp_w to generate contours as shown in Fig. 3(a). NEMO constructs the implicit connection graph by extracting all borders of contours (the dotted lines in Fig. 3(b)). In the propagation stage, NEMO performs the path propagation by identifying the adjacent *pseudo-maximum horizontally/vertically stripped tiles* (PMTs) of the last PMT in the minimum-cost path and then expanding the connected PMT list. The path propagation is repeated until the PMT containing the target is reached. Accordingly, NEMO generates routing wire segments by retracing the routing result and then places new wire segments on the layout. In Fig. 3(b), three PMTs are passed from S to T, and NEMO traces them to construct the final routing result.

C. Problem Formulation

***Problem** 1 (**TPL Aware Detailed Routing Problem**):* The minimum coloring spacing of TPL sp_{tp} indicates that two wire segments need to be assigned to different masks when their spacing is smaller than sp_{tp}. Given a netlist and sp_{tp}, the detailed routing for all nets is performed to minimize the number of stitches and TPL conflicts.

III. TECG

One conflict graph (CG) is used to maintain the *physical* coloring relations among all wire segments. The higher routed ratio, the higher complexity of CG. In Fig. 2(c), the decomposable layout is acquired only when D, G, and H are assigned to the identical color, which indicates that maintaining the consistent coloring relations among disconnected vertices in one CG can assist detailed routers in generating TPL-friendly results. However, maintaining certain coloring relations among non-adjacent vertices in one CG is quite difficult. Therefore, one *token graph* (TG) is proposed to maintain the *logical* coloring relation among sets of wire segments. Before introducing the proposed TG, the terminology of CG is defined as follows.

***Definition** 1 (**CG**):* A CG $\mathcal{G}^{\mathcal{C}} = (V^{\mathcal{C}}, E^{\mathcal{C}})$ contains a vertex set $V^{\mathcal{C}}$ representing all wire segments in one layer and an edge set $E^{\mathcal{C}}$

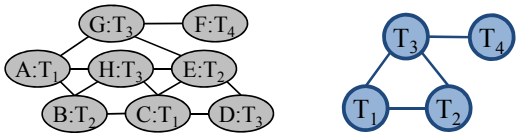

(a) (b)

Figure 4. TECG of layout in Fig. 2(c): (a) CG; (b) TG.

representing the minimum distance of two vertices, $v_i^c \in V^{\mathcal{C}}$, $v_j^c \in V^{\mathcal{C}}$, and $i \neq j$, is smaller than sp_{tp}.

***Definition** 2 (**Token**):* A token represents a potential color. Each vertex $v_i^c \in V^{\mathcal{C}}$ is assigned a token T to represent its potential color, denoted as $token(v_i^c) = T$. Each token T contains a CG vertex set, denoted as $V_t^{\mathcal{C}}(T) \subset V^{\mathcal{C}}$ where $\forall v_j^c \in V_t^{\mathcal{C}}(T), token(v_j^c) = T$, to indicate all vertices in $V_t^{\mathcal{C}}(T)$ is assigned to T.

***Definition** 3 (**TG**):* A TG $\mathcal{G}^{\mathcal{T}} = (V^{\mathcal{T}}, E^{\mathcal{T}})$ comprises a vertex set $V^{\mathcal{T}}$ representing all tokens in one layer and an edge set $E^{\mathcal{T}}$. Each edge in $E^{\mathcal{T}}$ between two tokens, $T_i \in V^{\mathcal{T}}, T_j \in V^{\mathcal{T}}$ and $i \neq j$, represents that there exists at least one edge in $\mathcal{G}^{\mathcal{C}}$ between $V_t^{\mathcal{C}}(T_i)$ and $V_t^{\mathcal{C}}(T_j)$.

***Definition** 4 (**Strictly Colored Component (SCC)**):* One SCC is defined as one three-tuple (T_i, T_j, T_k) where $T_i \in V^{\mathcal{T}}, T_j \in V^{\mathcal{T}}$, and $T_k \in V^{\mathcal{T}}$ comprise one three-clique in $\mathcal{G}^{\mathcal{T}}$. TG may contain a set of SCCs.

***Definition** 5 (**TECG**):* A TECG $\mathcal{G}^{\mathcal{TC}}$ comprises one CG $\mathcal{G}^{\mathcal{C}}$ and one TG $\mathcal{G}^{\mathcal{T}}$. A CG/TG may comprise several connected components, and each component is a subgraph of CG/TG and named as CSG/TSG. TPL conflict can be detected by finding a conflicting edge $e^c \in E^{\mathcal{C}}$ between $v_i^c \in V^{\mathcal{C}}$ and $v_j^c \in V^{\mathcal{C}}$ where $token(v_i^c) = token(v_j^c)$.

The proposed TG enables detailed routers to maintain high coloring-flexibility. Instead of assigning physical colors into wire segments, tokens are used to represent the potential colors. Therefore, one TG may contain more than three tokens even when TPL provides only three colors in each layer. Figures 4 depicts the TECG of the layout in Fig. 2(c). In Fig. 4(a), A and C are assigned to T_1; B and E are assigned to T_2; D, G, and H are assigned to T_3; and F is assigned to T_4. The corresponding TG as shown in Fig. 4(b) contains four tokens, T_1, T_2, T_3, and T_4, and one SCC $scc = (T_1, T_2, T_3)$. Therefore, the coloring result in Fig. 2(c) can be obtained by assigning T_1, T_2, and T_3 to c_1, c_2, and c_3, respectively, while T_4 can be assigned to c_1 or c_2. Notably, the number of vertices and edges of TG is much less than that of CG.

A. Token Graph Reduction

The coloring relation between non-adjacent tokens may become consistent after inserting an edge in one TG. Merging these tokens can effectively compact TG to facilitate TPL conflict detection. Two disconnected tokens $T_w \in V^{\mathcal{T}}$ and $T_x \in V^{\mathcal{T}}$ are merged when there exists one SCC $scc = (T_x, T_y, T_z)$ in $\mathcal{G}^{\mathcal{T}}$ where T_y and T_z connect to T_w. After merging T_w and T_x, the adjacent tokens of T_w and T_x connect to the merged token, which conduces to further graph reduction.

Algorithm 1 depicts the algorithm of TG_Update with two connected tokens T_i and T_j. TG_Update finds if there exists one $scc_i = (T_i, T_{i1}, T_{i2}) \in S^{SCC}$ where T_j connects to T_{i1} but not T_{i2}. If scc_i exists, T_j and T_{i2} are merged (lines 1–3). Otherwise, TG_Update tries to merge T_i with one token in an existing SCC in a similar scenario (lines 5–7). When the above two conditions cannot be met, TG_Update finds if any SCC, such as $scc_{com} = (T_i, T_j, T_k) \in S^{SCC}$, contains T_i and T_j. If scc_{com} exists and T_i and T_j have an other common adjacent token T_{com}, T_k and T_{com} are merged (lines 9–11). If no tokens can be merged and T_i and T_j have one common adjacent token T_{com}, TG_Update generates one SCC, and recursively calls itself until no more tokens/SCCs can be merged/generated (lines 12–16).

Assume that T_w and T_x are merged into T_{mrg}. Let $V_{ad}^{\mathcal{T}}(T_w)$ and $V_{ad}^{\mathcal{T}}(T_x)$ be the adjacent vertex sets of T_w and T_x in $\mathcal{G}^{\mathcal{T}}$, respectively. After merging T_w and T_x, the adjacent vertex set of T_{mrg} is $V_{ad}^{\mathcal{T}}(T_{mrg}) = V_{ad}^{\mathcal{T}}(T_w) \cup V_{ad}^{\mathcal{T}}(T_x)$. Therefore, token merging reduces $|V^{\mathcal{T}}|$ and $|E^{\mathcal{T}}|$ by one and $|V_{ad}^{\mathcal{T}}(T_w)| + |V_{ad}^{\mathcal{T}}(T_x)| - |V_{ad}^{\mathcal{T}}(T_{mrg})|$, respectively. Notably, some redundant TG edges are removed after token merging, and the inserted edges of the merged token can further benefit in simplifying TG. Algorithm 2 displays the algorithm of merging two tokens T_w and T_x. Merging T_w and T_x into T_{mrg} requires $scc \in S^{SCC}$ being updated by replacing T_w or T_x by T_{mrg} (lines 1–5). The replacement may cause two SCCs to contain the same tokens, resulting in redundant SCCs. After updating SCCs, the redundant SCCs are removed, if any (line 7). The additional edges of the merged token can further assist in graph reduction. (lines 8–10).

Algorithm 1 TG_Update

Require: Two connected tokens $T_i \in V^{\mathcal{T}}$ and $T_j \in V^{\mathcal{T}}$, one SCC set S^{SCC}

1: Find $scc_i = (T_i, T_{i1}, T_{i2}) \in S^{SCC}$ such that T_j connects to T_{i1} but not T_{i2};
2: **if** scc_i exists **then**
3: Token_Merging(T_j, T_{i2});
4: **else**
5: Find $scc_j = (T_j, T_{j1}, T_{j2}) \in S^{SCC}$ such that T_i connects to T_{j1} but not T_{j2};
6: **if** scc_j exists **then**
7: Token_Merging(T_i, T_{j2});
8: **else**
9: Find $scc_{com} = (T_i, T_j, T_k) \in S^{SCC}$;
10: **if** scc_{com} exists **and** T_i and T_j have one common adjacent token $T_{com} \neq T_k$ **then**
11: Token_Merging(T_k, T_{com});
12: **else if** T_i and T_j have one common adjacent token T_{com} **then**
13: Generate $scc_{new} = (T_i, T_j, T_{com})$;
14: $S^{SCC} := S^{SCC} \cup scc_{new}$;
15: TG_Update(T_i, T_j);
16: **end if**
17: **end if**
18: **end if**

Algorithm 2 Token_Merging

Require: $T_w \in V^{\mathcal{T}}$, $T_x \in V^{\mathcal{T}}$, one SCC set S^{SCC}

1: Merge T_w and T_x into T_{mrg};
2: **for all** $scc \in S^{SCC}$ **do**
3: **if** scc contains T_w or T_x **then**
4: Update scc by replacing T_w or T_x by T_{mrg};
5: **end if**
6: **end for**
7: Remove redundant SCC from S^{SCC};
8: **for all** token $t \in \{V_{ad}^{\mathcal{T}}(T_{mrg}) - \{V_{ad}^{\mathcal{T}}(T_w) \cap V_{ad}^{\mathcal{T}}(T_x)\}\}$ **do**
9: TG_Update(T_{mrg}, t);
10: **end for**

Algorithm 3 TECG_Update

Require: $\mathcal{G}^{\mathcal{TC}}$, $v_i^c \in V^{\mathcal{C}}$ and $v_j^c \in V^{\mathcal{C}}$ to be connected
1: Connect v_i^c and v_j^c in $\mathcal{G}^{\mathcal{C}}$;
2: **if** $token(v_i^c) = token(v_j^c)$ **then**
3: Detect one TPL conflict;
4: **else if** $token(v_i^c)$ and $token(v_j^c)$ are disconnected in $\mathcal{G}^{\mathcal{T}}$ **then**
5: Connect $token(v_i^c)$ and $token(v_j^c)$;
6: TG_Update($token(v_i^c)$, $token(v_j^c)$);
7: **end if**

B. TECG Update

In the routing stage, the vertices representing routing wire segments are inserted into one CG, and new tokens are generated in one TG to represent the potential colors of routing wire segments. When $v_i^c \in V^{\mathcal{C}}$ and $v_j^c \in V^{\mathcal{C}}$ are connected by an edge, an edge in one TG between $token(v_i^c)$ and $token(v_j^c)$ needs to be generated, if necessary. Algorithm 3 shows TECG_Update by connecting $v_i^c \in V^{\mathcal{C}}$ and $v_j^c \in V^{\mathcal{C}}$. Firstly, v_i^c and v_j^c are connected (line 1). One TPL conflict is detected when $token(v_i^c)$ and $token(v_j^c)$ are identical (lines 2–3). If $token(v_i^c)$ and $token(v_j^c)$ in the TG are disconnected, $token(v_i^c)$ and $token(v_j^c)$ are connected, and then *TG_Update* is used to compact the TG, if possible (lines 4–6).

Figure 5(a) depicts one TECG with one CG containing seven vertices, one TG containing seven vertices and ten edges, and two SCC $scc_1 = (T_1, T_2, T_7)$ and $scc_2 = (T_3, T_4, T_5)$. Connecting C and G (the dashed line) in the CG generates the connection between T_3 and T_7 (the dashed line) in the TG. Therefore, TG_Update(T_3, T_7) merges T_1 and T_3 into $T_{1'}$, and the two SCCs are updated by replacing T_1 and T_3 with $T_{1'}$ as shown in Fig. 5(b). Next, because T_5 is not a common adjacent token of T_1 and T_3 in Fig. 5(a), TG_Update$(T_{1'}, T_5)$ merges T_2 and T_5 into $T_{2'}$ followed by updating SCCs by replacing T_2 and T_5 with $T_{2'}$ as shown in Fig. 5(c). Similarly, T_4 is not a common adjacent token of T_2 and T_5 in Fig. 5(c) so TG_Update$(T_4, T_{2'})$ updates TG as shown in Fig. 5(d). Notably, after replacing T_4 and T_7 with $T_{3'}$, the three tokens of two SCCs become identical, requiring removing one redundant SCC. Therefore, one SCC is removed as shown in Fig. 5(d). Finally, TG_Update$(T_{2'}, T_6)$ is called because T_6 is not a common adjacent token of T_2 and T_5 in Fig. 5(b). Figures 5(e) depicts the updated TECG with one SCC $(T_{1'}, T_{2'}, T_{4'})$ where the assigned token of each vertex in CG is also updated. Notably, before connecting C and G in the CG, the number of TG vertices, TG edges, and SCCs are seven, ten, and two, respectively. After connecting C and G in CG, the number of TG vertices, TG edges, and SCCs are reduced by four, seven, and one, respectively, which indicates the proposed graph reduction technique effectively reduces the complexity of the TG. Therefore, the graph reduction technique of TECG can significantly reduce the complexity of the TPL conflict detection.

C. Implicit Edge in TG

Two tokens cannot be assigned to the same color when they connect to each other in one TG. We observe that two non-adjacent vertices in one TG cannot be assigned to one color when certain topology appears in TG. Notably, there might be other patterns that are not observed. An *implicit TG edge* between two non-adjacent tokens, such as T_i and T_j, is generated when all the following conditions are satisfied:

1) TG contains two SCCs (T_x, T_y, T_z) and (T_p, T_q, T_r), where
2) T_x and T_p connect to each other;

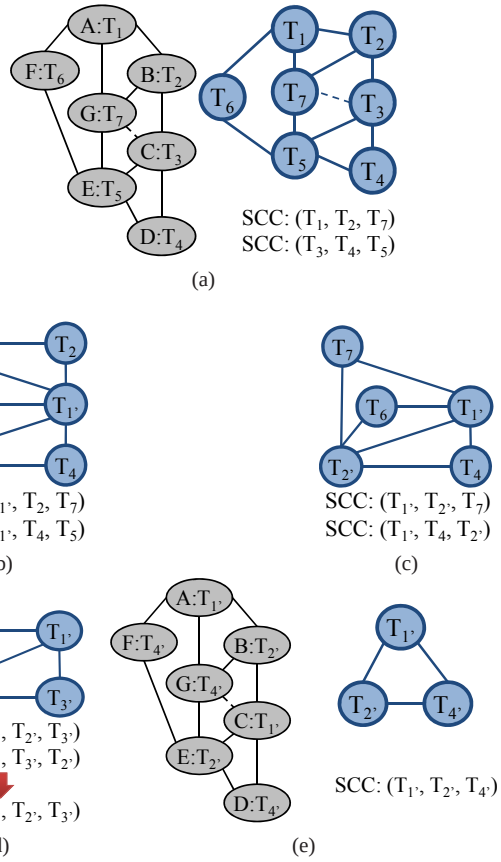

Figure 5. Example of TECG update: (a) TECG before connecting C and G in CG with two SCCs (T_1, T_2, T_7) and (T_3, T_4, T_5); (b) updated TG after merging T_1 and T_3 in (a) into $T_{1'}$; (c) updated TG after merging T_2 and T_5 in (b) into $T_{2'}$; (d) updated TG after merging T_4 and T_7 in (c) into $T_{3'}$; (e) updated TECG after merging $T_{3'}$ and T_6 in (d) into $T_{4'}$.

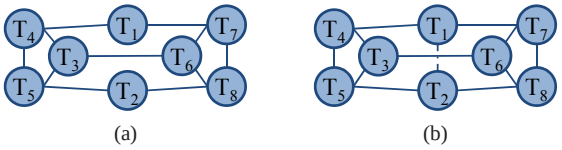

Figure 6. Example of implicit TG edge: (a) T_1 and T_2 are disconnected in TG; (b) implicit TG edge between T_1 and T_2 is inserted to indicate that colors of T_1 and T_2 must differ.

3) T_i connects to both T_y and T_q; and
4) T_j connects to both T_z and T_r.

Without loss of generality, there are three colors (c_1, c_2, c_3) can be used to color all tokens in one TG. Figure 6(a) depicts one TG contains the specific topology with two SCCs $scc_1 = (T_3, T_4, T_5)$ and $scc_2 = (T_6, T_7, T_8)$. Suppose that T_1 and T_2 are assigned to c_1. Notably, T_4/T_5 and T_7/T_8 can only be assigned to c_2 and c_3 due to the connection to T_1/T_2, resulting in that T_3/T_6 must be assigned to c_1. However, there exists one edge between T_3 and T_6. Therefore, T_1 and T_2 must be assigned to different colors, and one implicit edge is generated between T_1 and T_2 as shown in Fig. 6(b). In TECG_Update, after TG_Update (Algorithm 3: line 6),a set of implicit TG edges IE is generated by checking if the above conditions are satisfied. For each implicit edge $ie \in IE$, TG_Update checks if the TG can be further reduced by inserting ie.

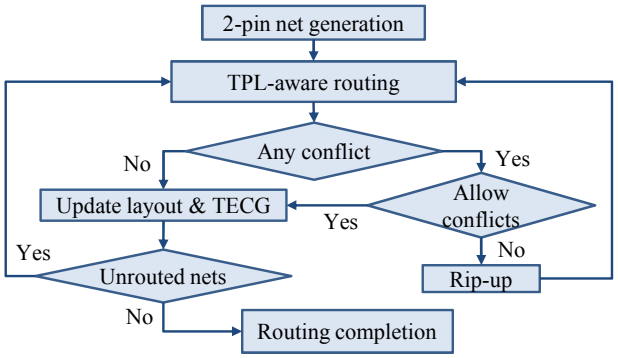

Figure 7. Overall flow of TRIAD.

IV. TRIAD

The TPL aware detailed router (TRIAD) focuses on accomplishing detailed routing for all given nets and generating a highly decomposable routing outcome with low yield loss. The routing model of NEMO is adopted here [14] [15]. This work proposes a technique to make TECG work on the routing model of NEMO. With the aid of TECG, TRIAD can generate stitches which cannot be generated by adopting the conventional DPL stitch generation scheme. Therefore, TRIAD can update the routing cost based on the number of stitches and TPL conflicts. Figure 7 shows the routing flow of TRIAD. Firstly, all multi-pin nets are decomposed into two-pin nets. A TPL-aware routing which allows the stitch generation at the cost of increasing routing cost is applied to route all two-pin nets. If one two-pin net is routed without any conflicts, then the layout and TECG are updated. Otherwise, TRIAD checks whether conflicts can be generated in current iteration while TRIAD is prohibited to generate TPL conflicts in the first few iterations. If the TPL stitch generation is not allowed, TRIAD rips up routed nets to release the routing resource and then re-routes the two-pin net. Otherwise, the layout and the TECG are directly updated.

A. TECG on the Gridless Routing Model

When constructing contours for routed wire segments, TRIAD also constructs *shadows* for routed wire segments presented by vertices in $\mathcal{G}^{\mathcal{C}}$. One shadow denotes the TPL effect region of its attached routed wire segment. TRIAD constructs shadows by extending routed nets by $hw_w + sp_{tp}$. Figure 8(a) shows three extracted PMTs with intersected shadows. The vertices in $\mathcal{G}^{\mathcal{C}}$ attached to the corresponding shadows assist TRIAD in detecting TPL conflicts when the potential routing wire segments pass through a PMT. The CG vertex representing the potential routing wire segment connects to the CG vertices representing routed wire segments by passing through their corresponding shadows, and the path propagation of TRIAD thus becomes aware of TPL conflicts. Figures 8(b)–(d) illustrate the path propagation of TRIAD. Figure 8(b) shows five routed wire segments, a PMT with three shadows, and one TECG. In Fig. 8(b), one routing wire segment passes through the PMT, sequentially inserting one vertex F in $\mathcal{G}^{\mathcal{C}}$ and one token T_4 in $\mathcal{G}^{\mathcal{T}}$. The routing wire segment represented by F passes through three shadows of A, B, and C. Therefore, TRIAD iteratively connects F to A, B, and C. After connecting F to A and B, T_1 and T_3 are merged into T_5 as shown in Fig. 8(c). In Fig. 8(d), TRIAD detects one TPL conflict by connecting F and C because $token(F)$ and $token(C)$ equal T_5.

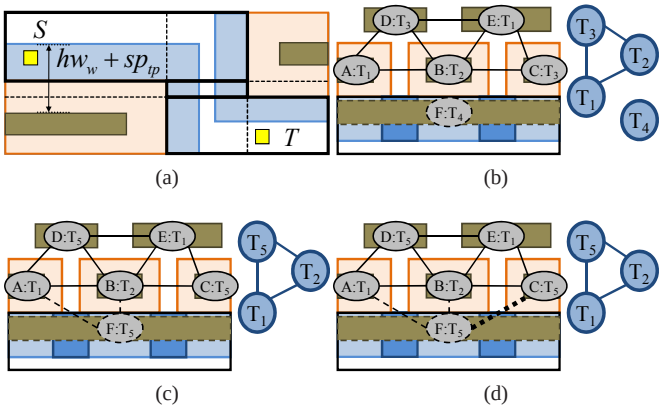

Figure 8. TECG on routing model of NEMO: (a) TRIAD constructs shadows to represent TPL effect region of routed wire segments; (b) PMT contains three shadows of three routed wire segments with TECG, and TRIAD inserts one vertex F in $\mathcal{G}^{\mathcal{C}}$ and a token T_4 in $\mathcal{G}^{\mathcal{T}}$ to represent the routing wire; (c) connecting F to A and B iteratively merges T_3 and T_4 into T_5; (d) TRIAD detects one coloring conflict after connecting F and C.

B. TPL Stitch Generation Scheme

After detecting TPL conflicts, TRIAD splits one of the terminal vertices of the conflicting edge to differ the assigned token by generating stitches, if possible. The DPL stitch generation scheme inserts one stitch in one wire when the wire contains at least one segment that is not passed by shadows of other wire segments. Based on the DPL stitch generation scheme, in Fig. 8(d), no stitch can be inserted in the routing wire segment because the routing wire segment is entirely overlapped by the shadows of routed wire segments. However, the TPL stitch generation scheme is quite different from the DPL stitch generation scheme. With the assistance of TECG, TRIAD can generate stitches at the wire segment even if which is entirely passed by shadows of other wires. Before introducing the proposed TPL stitch generation scheme, some definitions are given in the following.

***Definition** 6 **(Shadowy Interval)**:* One shadowy interval, denoted as φ, is one interval of one wire segment, and one wire segment may contain several shadowy intervals. Let $S^T_{shd}(\varphi)$ be the set of tokens represented by the shadow set passing through φ. For any two adjacent shadowy intervals φ_i and φ_j, $S^T_{shd}(\varphi_i)$ and $S^T_{shd}(\varphi_j)$ cannot be identical.

***Definition** 7 **(Splittable Shadowy Interval)**:* Given one wire segment *w* represented by one CG vertex v^c and one SCC $scc \in S^{SCC}$ containing $token(v^c)$. Let φ_i and φ_j be two adjacent shadowy intervals of w. One shadowy interval φ_i is called *splittable* when $|S^T_{shd}(\varphi_i) \cap S^T_{shd}(\varphi_j) \cap scc|$ is less than two.

***Definition** 8 **(Splittable CG Vertex)**:* Let $V^{\mathcal{C}}_{adj}(v^c)$ denote the adjacent vertex set of one vertex $v^c \in V^{\mathcal{C}}$. Given one SCC $scc = (token(v^c), token(v_{ad1}), token(v_{ad2})) \in S^{SCC}$ where $v^c_{ad1} \in V^{\mathcal{C}}_{adj}(v^c)$, $v^c_{ad2} \in V^{\mathcal{C}}_{adj}(v^c)$, and $v^c_{ad1} \neq v^c_{ad2}$. One CG Vertex v^c is called *splittable* when v^c contains a set of splittable shadowy intervals that can split v^c into a CG vertex set $V^{\mathcal{C}}_{SPLIT}$ where $\forall v^c_s \in V^{\mathcal{C}}_{SPLIT}, token(v^c_s)$ connects to at most two tokens of scc.

One wire segment to be split represented by one CG vertex v^c may contain several splittable shadowy intervals for one SCC. Generating stitches at all splittable shadowy intervals introduces unnecessary

Algorithm 4 TPL Stitch Generation

Require: One CG vertex v^c to be split, one CG vertex set $V_c^{\mathcal{C}}(v^c)$ adjacent to v^c where $\forall v_{adj}^c \in V_c^{\mathcal{C}}(v^c), token(v^c) = token(v_{adj}^c) = T_c$, one SCC scc containing T_c

1: Compute shadowy intervals S^{splt} in wire segments represented by v^c for scc;
2: **for all** Shadowy interval $\varphi \in S^{splt}$ **do**
3: **if** $|S_{shd}^T(\varphi)| > 2$ **then**
4: Increase the routing cost by one $penalty_{unsolvable}$;
5: **break**;
6: **end if**
7: **end for**
8: $num_{st} := 0$;
9: $\varphi_{st_cand} := \varphi_{st} := NULL$;
10: $S_{passed}^T := \emptyset$;
11: Topologically sort S^{splt};
12: **for all** Shadowy interval $\varphi \in S^{splt}$ **do**
13: **if** $|S_{shd}^T(\varphi)| = 1$ **then**
14: $\varphi_{st_cand} := \varphi$;
15: **end if**
16: $S_{passed}^T := S_{passed}^T \cup S_{shd}^T(\varphi)$;
17: **if** $|S_{passed}^T| > 2$ **then**
18: Generate one stitch at φ_{st_cand};
19: $++num_{st}$;
20: $S_{passed}^T := \emptyset$;
21: **for all** Shadowy interval φ_{passed} between φ and φ_{st} **do**
22: $S_{passed}^T := S_{passed}^T \cup S_{shd}^T(\varphi_{passed})$;
23: **end for**
24: $\varphi_{st} := \varphi_{st_cand}$;
25: **end if**
26: **end for**
27: Increase the routing cost by $num_{st} \times penalty_{st}$;

stitches, sequentially degrading the yield. To minimize the number of required stitches, the TPL stitch generation algorithm is proposed in Algorithm 4. All shadowy intervals S^{splt} in wire segments represented by v^c are firstly computed (line 1). One conflicting edge cannot be solved by splitting one wire segment with one shadowy interval passed by more than two shadows because two adjacent CG vertices must be assigned to the same token after splitting. After detecting one unsolvable conflicting edge, the routing cost is directly increased by one unsolvable penalty $penalty_{unsolvable}$ (lines 2–7). One token set S_{passed}^T is initially set as empty (line 10). Before generating stitches based on S^{splt}, S^{splt} is firstly topologically sorted (line 11), followed by sequentially checking the shadowy interval $\varphi \in S^{splt}$. If $|S_{shd}^T(\varphi)|$ equals one, φ is recorded as the potential position φ_{st_cand} to generate one stitch (lines 13–15). Inserting $S_{shd}^T(\varphi)$ into S_{passed}^T (line 16) may cause $|S_{passed}^T|$ to exceed two, requiring generating one stitch at φ_{st_cand} (lines 17–19). Then S_{passed}^T is set as empty, and the tokens attached to shadows passing through the shadowy intervals between φ_{st} and φ are inserted into S_{passed}^T (lines 20–23). Finally, φ_{st} is set as φ_{st_cand} to record the latest stitch position (line 24). After all shadowy intervals in S^{splt} are checked, the routing cost is increased based on the number of generated stitches (line 27). Notably, the token T_c that causes conflicting edges may belong to more than one SCC. Therefore, Algorithm 4 is applied to each SCC that contains T_c to generate necessary stitches.

Figures 9(a) and 9(c) show a small part of one TECG where CG vertices A, B, C, D and U represent four routed wire segments and

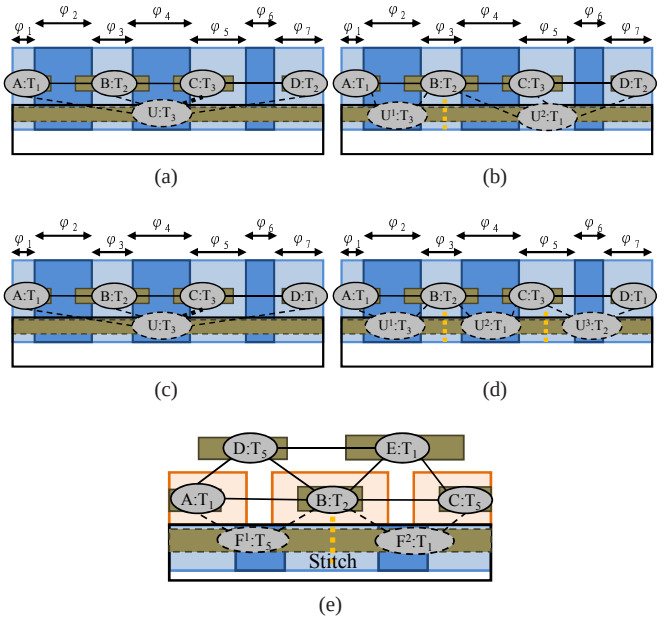

Figure 9. Example of TPL stitch generation schemes: (a)(c) DPL stitch generation scheme cannot insert any stitch; (b) generating one stitch can solve the conflict edge in (a); (d) generating two stitch can solve the conflict in (c); (e) TPL stitch generation of Fig. 8(d).

Table I
STATISTICS OF BENCHMARKS

Circuit	Size (μm^2)	# Layer	# Net	# 2Pin Net	# Pin
s5378	217.5 × 119.5	3	1694	3124	4818
s9234	202.0 × 112.5	3	1486	2774	4260
s13207	330.0 × 182.5	3	3781	6995	10776
s15850	352.5 × 194.5	3	4472	8321	12793
s38417	572.0 × 309.5	3	11309	21035	32344
s38584	647.5 × 336.0	3	14754	28177	42931

one routing wire segment, respectively. Notably, $token(A)$ equals T_1; $token(B)$ and $token(D)$ equal T_2/T_1; and $token(C)$ and $token(U)$ equal T_3 in Fig. 9(a)/(c). The routing wire segment in Fig. 9 contains seven shadowy intervals $\varphi_1, \varphi_2, \cdots$, and φ_7, and Algorithm 4 generates stitches by sequentially checking these shadowy intervals. In Fig. 9(a), $|S_{passed}^T|$ equals three when checking φ_4, resulting in generating one stitch at φ_3 as shown in Fig. 9(b). However, if $token(D)$ is assigned to T_1 as shown in Fig. 9(c), the edge (D, U^2) in Fig. 9(b) becomes conflicting. Similarly, for the TECG in Fig. 9(c), one stitch is generated in φ_3 as shown in Fig. 9(d) followed by setting S_{passed}^T as $\{T_2, T_3\}$. When checking φ_7, S_{passed}^T equals $\{T_1, T_2, T_3\}$, requiring generating another stitch at φ_5 as shown in Fig. 9(d). To solve the conflicting edge in Fig. 8(d), one stitch is generating at the routing wire segment by splitting F into F^1 and F^2 as shown in Fig. 9(e).

V. EXPERIMENTAL RESULTS

The algorithm herein was implemented in C++ language on a workstation with 4-Core 2.4 GHz CPU and 82GB memory. A total six benchmarks [18] are adopted in this work. We scale all benchmarks, including routing area and features size, to approach the target process node. Table I shows the corresponding statistics. The minimum resolution (half-pitch) for pushing the 193*nm* lithography's

Table II
COMPARISON BETWEEN WIRELENGTH, STITCHES, CONFLICTS, AND RUNTIME OF THE GREEDY APPROACH (GREED) AND TRIAD

Circuit	Wirelength (nm)		# Stitch		# Conflict		Runtime (s.)	
	GREEDY	DPLAG	GREEDY	DPLAG	GREEDY	DPLAG	GREEDY	DPLAG
s5378	382900	381170	165	0	0	0	9.47	14.36
s9234	286503	284608	157	0	1	0	8.62	9.78
s13207	910055	903705	405	1	2	0	25.38	49.11
s15850	1131665	1124715	371	0	2	0	40.83	95.80
s38417	2457675	2461940	1528	0	3	0	122.7	443.75
s38584	3211985	3204160	1264	2	2	0	168.97	660.38
Ave.	100%	99.46%	560.67	0.50	-	-	1	2.41

single exposure limit is around 40*nm*. Thus, to print 20*nm* half-pitch, we need double patterning, and to print 10*nm* half-pitch, we need quadruple patterning. The minimum coloring spacing for single exposure lithography is fixed, i.e., around 40*nm*. The purpose of multiple patterning is to push for smaller resolution (half-pitch). Therefore, to the first order, the minimum coloring spacing would be *n* times minimum wire spacing (i.e., half-pitch) of the *n* patterning lithography. The minimum coloring spacing sp_{tp} is set as three times of the minimum wire spacing.

As there is no other TPL aware router published, to demonstrate the effectiveness of the proposed algorithm, a greedy approach (GREED) is developed based on TRIAD for comparison. GREED only contains three colors for each layer and greedily determines the colors of routing wire segments. In GREED, the colors of routed wire segments are fixed. GREED adopts the same routing flow of TRIAD without TECG. Notably, TRIAD and GREED are prohibited to generate conflicts in the first fifteen iterations for fair comparison. Table II shows the wirelength, the number of stitches (# Stitch), the number of unsolvable conflicts (# Conflict), and runtime of GREED and TRIAD. TRIAD produces no conflicts in all cases and only introduces one and two stitches in $s13207$ and $s38548$, respectively, while GREED only generates conflict-free results in one case with total 3890 stitches. Moreover, the average wirelength of TRIAD is less than that of GREED by 0.54% because GREED has to detour the routed colored wire segments to avoid generating TPL conflicts. Thus, GREED requires more detours than TRIAD does. Compared to GREED, TRIAD can generate conflict-free results in all cases at the cost of an average 2.41× of runtime. For the largest case $s38584$, the runtime of TRIAD is less than four times of that of GREED. The most runtime spends of the graph reduction which provides TRIAD high coloring-flexibility to generate TPL-friendly results.

VI. CONCLUSION

The detailed routing is a key optimization stage for TPL. To effectively detect TPL conflicts with high coloring-flexibility, this work proposes a token graph-embedded conflict graph (TECG) with a graph reduction technique. This work develops a TPL aware detailed router (TRIAD) with the TPL stitch generation to solve TPL conflicts.. With the aid of TECG, TRIAD can generate stitches in one wire even when the wire is entirely intersected by the TPL effect regions of other wires. Experimental results show that the routing results have no TPL conflicts and introduces total three stitches for two cases with 0.54% decrement in wirelength at the cost of 2.41× of runtime. The future work focuses on the density-driven TPL aware detailed routing.

REFERENCES

[1] Y. Du, H. Zhang, M. D. F. Wong, and K.-Y. Chao, "Hybrid lithography optimization with e-beam and immersion processes for 16nm 1D gridded design," in *17th Asia and South Pacific Design Automation Conference (ASP-DAC)*, Feb. 2012, pp. 707–712.

[2] A. B. Kahng, "Key directions and a roadmap for electrical design for manufacturability," in *37th European Solid State Device Research Conference*, Sept. 2007, pp. 83–88.

[3] Y. Borodovsky, "Lithography 2009 overview of opportunities," in *Semicon West*, San Francisco, CA, USA, July 2009.

[4] M. Cho, Y. Ban, and D. Z. Pan, "Double patterning technology friendly detailed routing," in *Proc. of Intel. Conf. on Computer-Aided Design*, 2008, pp. 506–511.

[5] X. Gao and L. Macchiarulo, "Enhancing double-patterning detailed routing with lazy coloring and within-path conflict avoidance," in *Proc. of Conf. on Design, Automation and Test in Europe*, 2010, pp. 1279–1284.

[6] Y.-H. Lin and Y.-L. Li, "Double patterning lithography aware gridless detailed routing with innovative conflict graph," in *Proc. of Design Automation Conference*, 2010, pp. 398–403.

[7] K. Yuan and D. Z. Pan, "WISDOM: Wire spreading enhanced decomposition of masks in double patterning lithography," in *Proc. of Intel. Conf. on Computer-Aided Design*, 2010, pp. 32–38.

[8] C. Cork, J.-C. Madre, and L. Barnes, "Comparison of triple-patterning decomposition algorithms using aperiodic tiling patterns," in *Photomask and Next-Generation Lithography Mask Technology XV*, 2008.

[9] B. Yu, K. Yuan, B. Zhang, D. Ding, and D. Z. Pan, "Layout decomposition for triple patterning lithography," in *Proc. of Intel. Conf. on Computer-Aided Design*, 2011, pp. 1–8.

[10] Y. Chen, P. Xu, L. Miao *et al.*, "Self-aligned triple patterning for continuous ic scaling to half-pitch 15nm," in *SPIE*, 2011.

[11] B. Mebarki, H. D. Chen, Y. Chen *et al.*, "Innovative self-aligned triple patterning for 1x half pitch using single "spacer deposition-spacer etch" step," in *SPIE*, 2011.

[12] K. Lucas, C. Cork, B. Yu, G. Luk-Pat, B. Painter, and D. Z. Pan, "Implications of triple patterning for 14nm node design and patterning," in *SPIE Advanced Lithography Symposium Design for Manufacturability through Design-Process Integration VI*, 2012.

[13] A. B. Kahng, C.-H. Park, X. Xu, and H. Yao, "Layout decomposition approaches for double patterning lithography," *IEEE Trans. on Computer-Aided Design of Integrated Circuits and Systems*, vol. 29, no. 6, pp. 939–952, June 2010.

[14] Y.-L. Li, H.-Y. Chen, and C.-T. Lin, "NEMO: A new implicit-connection -graph-based gridless router with multilayer planes and pseudo tile propagation," *IEEE Trans. on Computer-Aided Design of Integrated Circuits and Systems*, vol. 26, no. 4, pp. 705–718, April 2007.

[15] Y.-N. Chang, Y.-L. Li, W.-T. Lin, and W.-N. Cheng, "Non-slicing floorplanning-based crosstalk reduction on gridless track assignment for a gridless routing system with fast pseudo-tile extraction," *ACM Trans. on Design Automation of Electronic Systems*, vol. 16, no. 2, March 2011.

[16] A. Margarino, A. Romano, A. De Gloria, F. Curatelli, and P. Antognetti, "A tile-expansion router," *IEEE Trans. on Computer-Aided Design of Integrated Circuits and Systems*, vol. 6, no. 4, pp. 507–517, July 1987.

[17] J. Cong, J. Fang, and K. Khoo, "DUNE: A multilayer gridless routing system," *IEEE Trans. on Computer-Aided Design of Integrated Circuits and Systems*, vol. 20, no. 5, pp. 633–646, May 2001.

[18] J. Cong, J. Fang, M. Xie, and Y. Zhang, "MARS - a multilevel full-chip gridless routing system," *IEEE Trans. on Computer-Aided Design of Integrated Circuits and Systems*, vol. 24, no. 3, pp. 382–394, March 2005.